

See discussions, stats, and author profiles for this publication at: <https://www.researchgate.net/publication/229534722>

# Tautomeric Forms of Adenine: Vertical Ionization Energies and Dyson Orbitals

ARTICLE *in* INTERNATIONAL JOURNAL OF QUANTUM CHEMISTRY · JANUARY 2009

Impact Factor: 1.43 · DOI: 10.1002/qua.22363

CITATIONS

20

READS

34

## 3 AUTHORS:



Raman K. Singh

University of Yamanashi

15 PUBLICATIONS 64 CITATIONS

SEE PROFILE



Joseph Vincent Ortiz

Auburn University

150 PUBLICATIONS 6,078 CITATIONS

SEE PROFILE



Manoj Mishra

Cranfield University

83 PUBLICATIONS 447 CITATIONS

SEE PROFILE

# Tautomeric Forms of Adenine: Vertical Ionization Energies and Dyson Orbitals

RAMAN K. SINGH,<sup>1</sup> J. V. ORTIZ,<sup>1,2</sup> MANOJ K. MISHRA<sup>1</sup>

<sup>1</sup>Department of Chemistry, Indian Institute of Technology Bombay, Powai 400 076, India

<sup>2</sup>Department of Chemistry and Biochemistry, Auburn University, Auburn, Alabama 36849-5312

Received 6 May 2009; accepted 13 May 2009

Published online 3 November 2009 in Wiley InterScience (www.interscience.wiley.com).

DOI 10.1002/qua.22363

**ABSTRACT:** For the MP2/6-311++g(2df,p) optimized geometry of all the 14 adenine tautomers, the first three vertical ionization energies have been calculated using several electron propagator decouplings. The corresponding Dyson orbitals provide detailed insight into the role of structural variations in different adenine tautomers. Changes in the electron binding energies and the corresponding Dyson orbital amplitudes have been correlated with tautomeric proton shifts and changes in conjugation patterns. © 2009 Wiley Periodicals, Inc. *Int J Quantum Chem* 110: 1901–1915, 2010

**Key words:** vertical ionization energies; electron propagator decouplings; Dyson orbital; electron binding energies

## 1. Introduction

Tautomers of nucleic acid bases are believed to be involved in many different biochemical processes, including point mutations [1, 2]. Their presence in biomolecules can alter cell functions and contribute to carcinogenic behavior [3–7]. In biological systems, nucleic acid bases are domi-

nantly present in the stable canonical form; however, the situation is different with gas-phase experiments where various tautomers coexist [8–17] and are believed to contribute to the anomalies in photoelectron [18–33], infrared [34], and nuclear magnetic resonance [35] spectral line shapes of nucleic acid bases. The study of nucleic acid base tautomers is therefore of obvious interest and has received considerable attention [1–36]. A recent theoretical study [16] of microhydration of adenine tautomers shows that the tautomers may also exist in water. Of the many tautomers of nucleic acid bases, those belonging to adenine have received particularly detailed attention since these tautomeric variants provide a structurally and energetically easy fit for mutagenic pairing with cytosine and thymine [37, 38]. As usual, the ionization po-

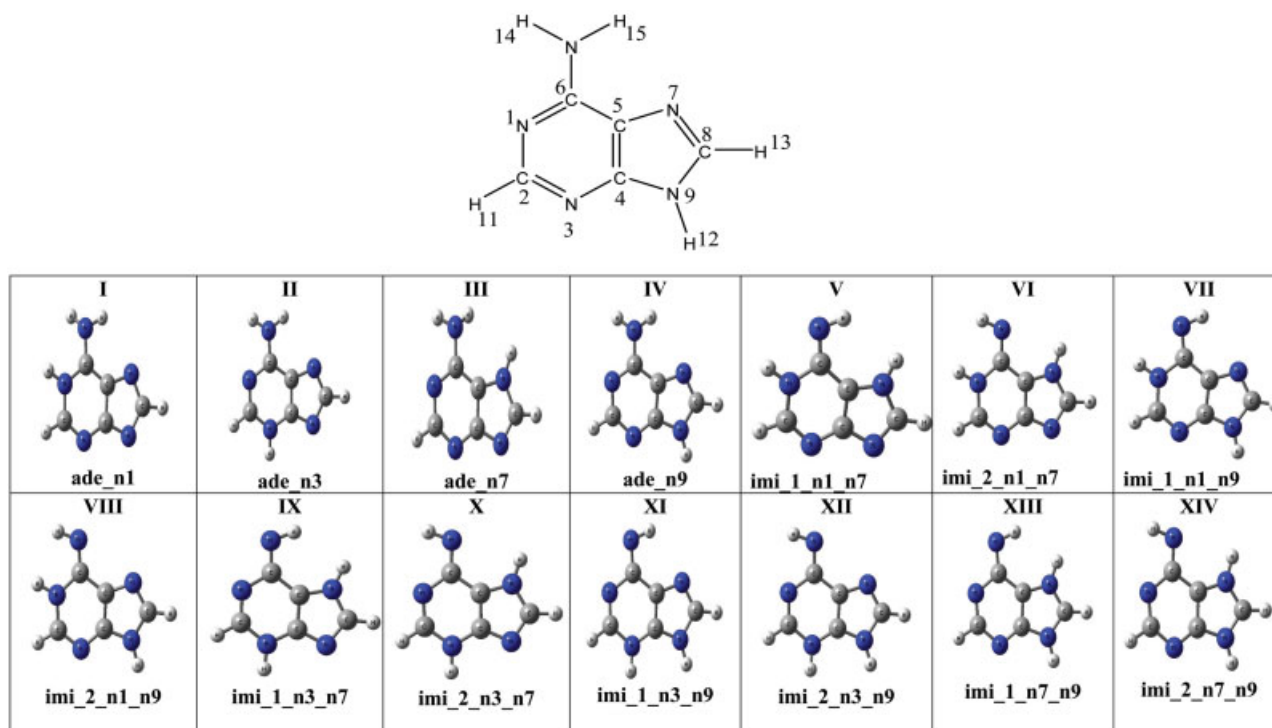
Correspondence to: J. V. Ortiz; e-mail: ortiz@auburn.edu or Manoj K. Mishra; e-mail: mmishra@iitb.ac.in

Contract grant sponsor: Department of Science and Technology, India.

Contract grant number: SR/S1/PC-30/2006.

Contract grant sponsor: the National Science Foundation, USA.

Contract grant number: CHE-0809199.



**FIGURE 1.** Canonical adenine (ade\_n9) and other tautomers. [Color figure can be viewed in the online issue, which is available at [www.interscience.wiley.com](http://www.interscience.wiley.com).]

tential being a critical discriminant of reactivity, experimental determination [27–35], and theoretical calculation [33, 37–45] of ionization energies of adenine tautomers have seen much recent activity. Photoelectron spectra (PES) of the canonical adenine base have been reported by many researchers [27–35] and some of the complications in the assignment of peaks have been attributed to the presence of possible tautomers [33, 40]. A reassignment of the four lowest cationic states of adenine has been proposed recently on the basis of time-resolved PES [46, 47].

One of the earliest attempts at theoretical resolution of adenine PES was through a semiempirical AM1 variant of the restricted open-shell Hartree-Fock (HF) and Outer Valence Green's function (OVGF) approaches that were used to get vertical and adiabatic ionization energies of a selected few tautomers of the adenine DNA base [40]. Guerra et al. [38] computed vertical and adiabatic first ionization energies of 12 adenine tautomers with BP86/TZ2P and BP86/QZ4P levels of density functional theory (DFT). Vertical ionization energies for the outer valence space of four neutral amino tautomers have been compared in detail at the BP86/

QZ4P and SAOP/QZ4P levels of DFT calculations [38]. The adenine bases have been shown to exist in 14 different tautomeric forms [16] by shifting one or two protons to a different nitrogen atom (see Fig. 1) and two additional tautomers are not covered by the DFT studies [38]. Also, for ionization from inner orbitals, use of DFT orbital energies as binding energies [38] is not so satisfactory. Multiconfigurational perturbative and coupled-cluster calculations seemed to predict the same order of  $\pi$  and  $\sigma$  final states, but quantitative agreement has not been obtained for all states [48]. A detailed analysis of the ionization energies of various adenine tautomers is therefore of obvious utility and importance.

In general, correlated calculation of ionization energies requires a separate calculation for the neutral target and each ionized state, with a small ionization energy being obtained as a difference between two large total energies. The use of the conventional correlated methods such as DFT, MP2, MCSCF, and CI for calculating ionization energies of all adenine tautomers is therefore not only computationally more demanding but also somewhat less satisfactory in comparison with the electron propagator theory [49–56] that provides verti-

cal electron binding energies for ionization from any orbital from a single calculation and permits systematic improvement in incorporation of correlation and relaxation effects. For these reasons, the electron propagator theory (EPT)-based methods have emerged as an economic, efficient, and reliable tool for direct computation of ionization energies from a single calculation [57, 58] and their use for investigation of adenine tautomers could offer an improved characterization of ionization energies and the effect of attendant structural changes in adenine tautomers. The electron propagator theory [53–55] is a computationally economic and accurate method for calculation of ionization energies and provides a framework for the systematic inclusion of electron correlation and orbital relaxation effects in a one-electron picture of molecular structure. The corresponding Dyson orbitals provide electronic structure interpretations that accompany electron attachment and detachment processes [57–59]. Dolgounitcheva et al. [41] calculated *ab initio* vertical ionization potentials of the natural adenine (ade\_n9) using OVGf [49, 50] and partial third-order (P3) approximants [51, 52] of the EPT [53–56] using 6-311G\*\*/cc-pVDZ basis sets. The P3 results were shown to provide close agreement with experimental values, and results from the 6-311G\*\* basis were adjudged to be most reliable [41]. The theoretical PES of adenine has also been calculated [33] using the third-order Algebraic-Diagrammatic Construction (ADC(3)) approximant [49, 50, 60] of EPT, and the ADC(3)/6-31G valence shell PES of adenine has been compared with experimental results and also those obtained using the OVGf approximant with a 6-311++G\*\* basis [33].

To the best of our knowledge, a systematic and comprehensive study of all 14 adenine tautomers using different EPT approximants has not been done so far. A detailed analysis of ionization energies for all the tautomers of adenine is of obvious biochemical importance and a comparative study of these tautomers using different decouplings of the electron propagator theory is the principle focus of this article. Variations in the corresponding Dyson orbitals as a function of the structural change in the tautomers to elicit the role of H-atom displacements in affecting ionization energies are an additional goal. These results, we hope, will assist in accurate assignment of PES, and for this purpose we have included vertical detachment energies even for adenine tautomers whose PES have not been ascertained experimentally so far. Dipole moments of these tautomers affect their interaction with other

molecules and the MP2/6-311++g (2df,p) values calculated by us for all 14 adenine tautomers are also compiled and analyzed.

The electron propagator theory [53–56] and its various decouplings [49–52, 57–60] are well documented and only a skeletal outline pertinent to our discussion is offered in the following section. The results are discussed in Section 3 and a summary of the main findings concludes this article.

## 2. Method

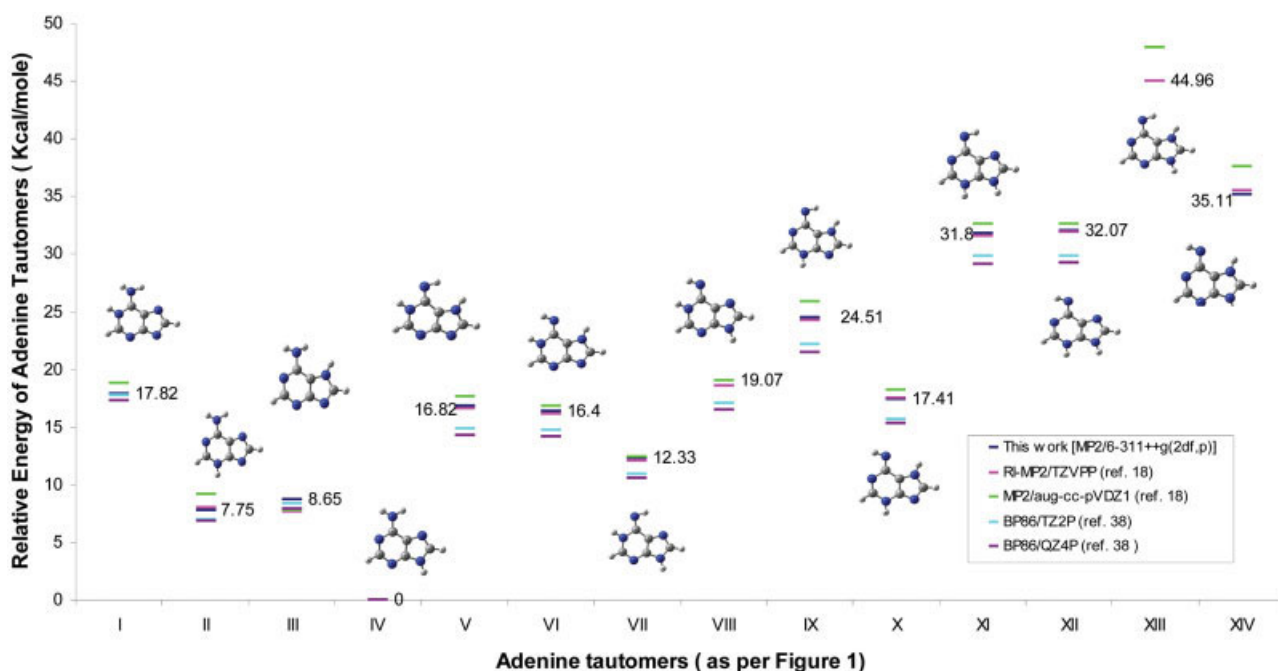
Electron propagator calculations for vertical electron detachment and attachment energies are based on the Dyson equation [57, 58]. The Dyson equation governing all electron propagator decouplings may be rewritten in the form of one-electron equations such that

$$[\hat{f} + \hat{\Sigma}(\varepsilon_i)]\phi_i^{\text{Dyson}}(x) = \varepsilon_i\phi_i^{\text{Dyson}}(x) \quad (1)$$

where  $\hat{f}$ , is the one-electron HF operator and  $\hat{\Sigma}(\varepsilon)$  is an energy-dependent nonlocal operator, the so-called self-energy [53]. This operator describes electron correlation and orbital relaxation effects that are neglected by the Fock operator,  $\hat{f}$ . Eigenfunctions of Eq. (1) are the Dyson orbitals,  $\phi_i^{\text{Dyson}}$ . For vertical electron detachment processes, the Dyson orbitals are given by

$$\phi_i^{\text{IP,Dyson}}(x_N) = \sqrt{N} \int \Psi_N(x_1, x_2, x_3, \dots, x_N) \times \Psi_{i,N-1}^*(x_1, x_2, x_3, \dots, x_{N-1}) dx_1 dx_2 \dots dx_{N-1}. \quad (2)$$

Here,  $\Psi_N(x_1, \dots, x_N)$  is the wavefunction for the  $N$ -electron, initial state and  $\Psi_{i,N\pm 1}(x_1, \dots, x_{N\pm 1})$  is the wave function for the  $i$ -th final state with  $N \pm 1$  electrons. In both expressions,  $x_j$  represents the space-spin coordinates of electron  $j$ . The eigenvalues,  $\varepsilon_i$ , of the Dyson equation correspond to electron binding energies of the molecular system. By using perturbative arguments [51], one may justify neglect of off-diagonal matrix elements of the self-energy operator in the HF basis. This leads to the simpler quasi-particle expression, also called the diagonal approximation [49–52, 57–59]. Thus, the electron binding energies in the quasi-particle approximation read  $\varepsilon_i^{\text{HF}} + \Sigma_{ii}(E) = E$ , where  $\varepsilon_i^{\text{HF}}$  is the  $i$ -th canonical, HF orbital energy. All EPT methods used in this articles are based on this class of ap-



**FIGURE 2.** Relative energy of adenine tautomers (kcal/mole). [Color figure can be viewed in the online issue, which is available at [www.interscience.wiley.com](http://www.interscience.wiley.com).]

proximation, namely, diagonal second and third order, P3 and OVGf [49–56, 60]. The pole strength,  $p_i$ , is a good indicator of the qualitative validity of this approximation. Because the pole strength is defined by

$$p_i = \int |\phi_i^{\text{Dyson}}(x)|^2 dx \quad (3)$$

the Dyson orbital [57, 58] within the diagonal approximation is simply proportional to a normalized, canonical HF orbital such that

$$\phi_i^{\text{Dyson}}(x) = \sqrt{P_i} \Psi_i^{\text{HF}}(x). \quad (4)$$

Thus, the pole strength takes values between zero and unity. If the ionization process is well described by a Koopmans (frozen-orbital) picture, pole strengths are very close to 1.0. When pole strengths are less than 0.8, nondiagonal analysis of energy poles is required. All pole strengths in this work exceed 0.8. Those that are below 0.85 are less reliable and therefore the corresponding electron binding energies are denoted by “\*”.

All computations were performed using the Gaussian03 suite of programs [61]. Geometry opti-

mizations and frequency calculations for adenine tautomers were performed at the MP2 level of theory with ++g(d,p), g(2df,p), and ++g(2df,p) basis sets and since the largest ++g(2df,p) basis set provides dipole moment value identical to the experimental value for the canonical ade\_n9 base, we have retained results from this basis for detailed discussion in the following sections. All structures have  $C_1$  symmetry with real and positive frequencies. The Dyson orbital pictures presented in the Tables were created with GaussView, and an isosurface value of 0.02 was used to produce these figures. Although results from many decouplings are presented, in furtherance of our application of the P3 decouplings to other biomolecules [62, 63], we have adopted the P3 results for ordering of orbitals such as HOMO, HOMO-1, and HOMO-2.

### 3. Results and Discussion

The relative stability of all the adenine tautomers is depicted in Figure 2 where, as expected, the canonical neutral adenine (ade\_n9) base (total energy =  $-466.4188$  a.u.) is the most stable among all tautomers. The tautomers ade\_n3 and ade\_n7 that have been reported [34] to be the most likely par-

**TABLE I**  
**Dipole moment of adenine tautomers.**

S.No.	Tautomers	Dipole moments (Debye)				Expt. [36]
		This work MP2/ 6-311 ++g (2df,p)	RI-MP2/TZVPP [16]	BP86/QZ2P[38] Cs (C <sub>1</sub> )	BP86/QZ4P[38] Cs (C <sub>1</sub> )	
I	ade_n1	8.9	8.8	9.0(8.4)	8.8(8.4)	2.5
II	ade_n3	4.7	4.7	4.0(4.0)	4.0(4.0)	
III	ade_n7	7.5	6.8	7.5(7.0)	7.3(7.0)	
IV	ade_n9	2.5	2.8	2.4(2.5)	2.3(2.3)	
V	imi_1_n1_n7	2.8	3.0	3.1	3.0	
VI	imi_2_n1_n7	3.4	3.6	3.5	3.3	
VII	imi_1_n1_n9	4.4	4.3	3.8	3.8	
VIII	imi_2_n1_n9	5.3	5.2	4.5	4.4	
IX	imi_1_n3_n7	5.3	5.2	4.6	4.5	
X	imi_2_n3_n7	3.4	3.2	2.8	2.9	
XI	imi_1_n3_n9	10.7	10.6	9.8	9.8	
XII	imi_2_n3_n9	10.2	10.1	9.4	9.3	
XIII	imi_1_n7_n9	12.3	12.4			
XIV	imi_2_n7_n9	9.5	9.5			

ticipants in spectral line broadening are energetically closest to the natural ade\_n9 base, with ade\_n3 and ade\_n7 being nearly degenerate. Similarly, the imino tautomer imi\_1\_n1\_n9 that has been reported to be the most likely candidate in the mutagenic adenine-cytosine pairing [38] is the most stable among imino tautomers. The two tautomers imi\_1\_n7\_n9 and imi\_2\_n7\_n9 whose ionization energies have not been calculated so far are energetically most removed from the natural ade\_n9 base. These are probably unlikely to be relevant to gas-phase spectra. However, because all the tautomers are within 2.18 eV of each other as far as total energies are concerned, even these may turn out to be important in their own way. As depicted in Figure 2, the relative stability compares well with the ordering reported by Hanus et al. [16] and Guerra et al. [38] and in general reflects the level of steric hindrance in different tautomers. The higher energy imino tautomers imi\_1\_n7\_n9 and imi\_2\_n7\_n9 possess zwitterion-like structures [16] and differ from each other through the opposite orientation of the imino hydrogen. As expected, these zwitterionic tautomers have very large dipole moments (Table I) and because the dipole moment is critical to various interactions (electrostatic, H-bonding, hydration, etc.), our MP2/6-311++g(2df,p) values for dipole moments of all the adenine tautomers along with those from other computations are collected in Table I. The dipole moment values and trends are similar to

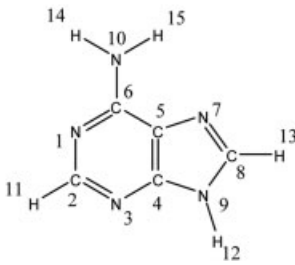

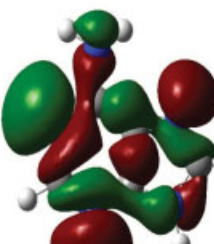

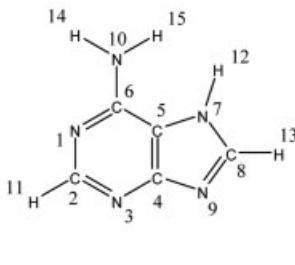
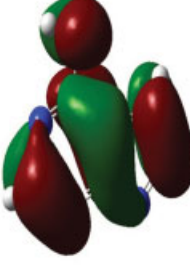
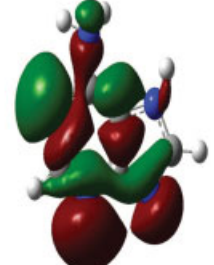

those discussed by Hanus et al. [16], and it is gratifying to note that our MP2/6-311++g(2df,p) dipole moment value for the canonical ade\_n9 offer closest agreement with the experimental value. The ionization energies from different EPT decouplings for HOMO, HOMO-1, and HOMO-2 of all the 14 tautomers using the 6-311++g(2df,p) basis set are presented in Tables II–VIII and are discussed below. Correlated calculations often change the sequence of final states. Corrections to Koopmans results are larger for  $\sigma$  orbitals than for  $\pi$  orbitals, and therefore the order of the final states that correspond to ionization from the HOMO-1 and HOMO-2 orbitals may be reversed. This will be seen to be a recurring feature for many adenine tautomers.

The ionization energies of the natural adenine ade\_n9 have been investigated both experimentally and computationally using a variety of methods and these results are collected in Table II. The P3 EPT result provides closest agreement and our results for ionization from HOMO, HOMO-1, and HOMO-2 are quite close to the experimental values. Even though the results of Koopmans theorem (KT) are close to the experimental values for ionization from the HOMO, the wrong ordering, as also the large deviation from experimental values for HOMO-1 and HOMO-2 seen in KT results, point to the need for correlated EPT decouplings like P3 for accurate resolution of PES. Results computed using other approaches have somewhat uneven scatter



TABLE II

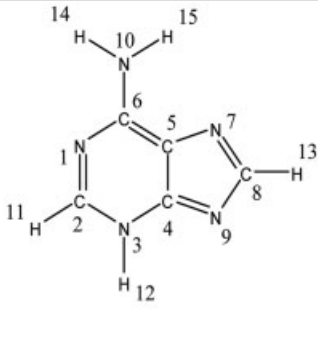
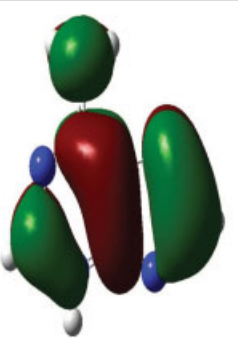
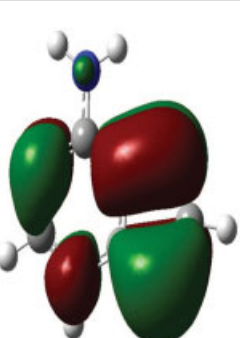
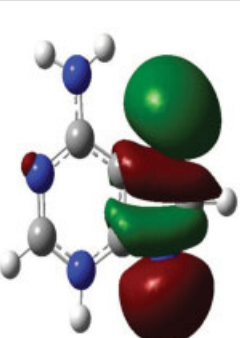
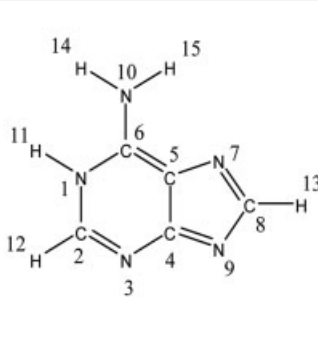
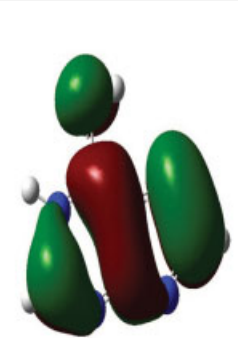
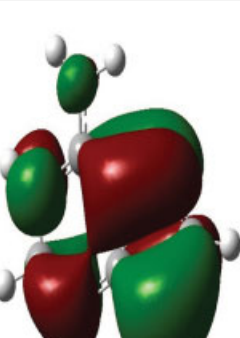
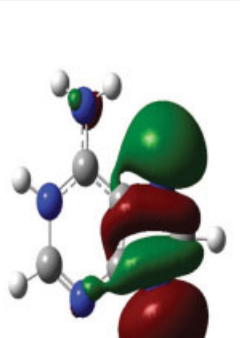
Vertical electron detachment energies of ade\_n9 and ade\_n7 tautomers with corresponding Dyson Orbitals. [Color figure can be viewed in the online issue, which is available at [www.interscience.wiley.com](http://www.interscience.wiley.com).]

 <p style="text-align: center;"><b>ade_n9</b></p>	 <p style="text-align: center;"><b>HOMO</b></p>	 <p style="text-align: center;"><b>HOMO-1</b></p>	 <p style="text-align: center;"><b>HOMO-2</b></p>
KT	8.38	11.15	10.18
2 <sup>nd</sup> Order	8.10	8.40	9.11
3 <sup>rd</sup> Order	8.48	10.30	9.84
OVGF	8.37	9.53	9.47
P3	8.64	9.67	9.79
Expt.[33]	8.48	9.45	9.54
ADC(3)[33]	7.93	9.20	9.36
$\Delta$ SCF[40]	8.53		
HF/MP2	7.45/9.38		
6-31++g(d,p)[37]			
PHF/PMP2	7.36/8.62		
6-31++g(d,p)[37]			
BP86/TZ2P[38]	8.27		
BP86/QZ4P[38]	8.18		
OVGF/TZVP[38]	8.20		
DFT-GGA[42]	8.23		
 <p style="text-align: center;"><b>ade_n7</b></p>	 <p style="text-align: center;"><b>HOMO</b></p>	 <p style="text-align: center;"><b>HOMO-1</b></p>	 <p style="text-align: center;"><b>HOMO-2</b></p>
KT	8.72	11.07	9.87
2 <sup>nd</sup> Order	8.27	8.27*	9.03
3 <sup>rd</sup> Order	8.73	10.29	9.69
OVGF	8.60	9.49	9.35
P3	8.84	9.58	9.68
$\Delta$ SCF[40]	8.93		
BP86/TZ2P[38]	8.48		
BP86/QZ4P[38]	8.39		
OVGF/TZVP[38]	8.26		

\*Pole strength less than 0.85.

TABLE III

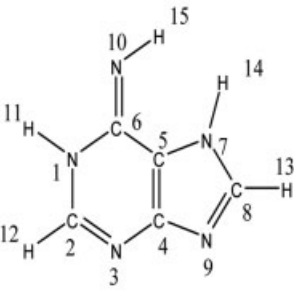
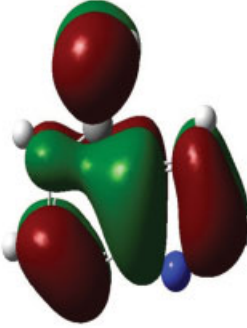
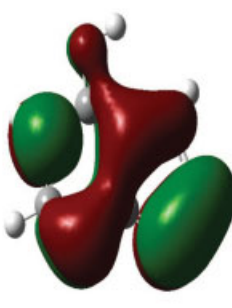
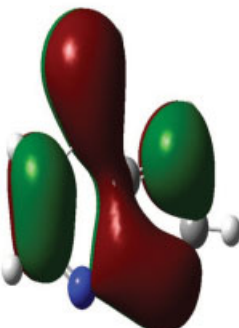
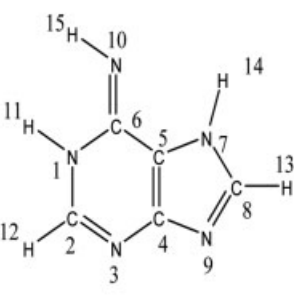
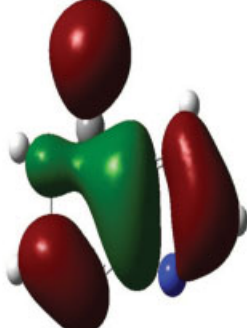
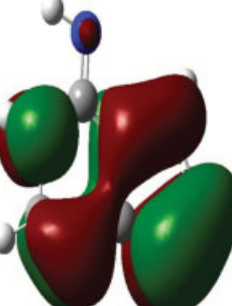

Vertical electron detachment energies of ade\_n3 and ade\_n1 tautomers with corresponding Dyson orbitals. [Color figure can be viewed in the online issue, which is available at [www.interscience.wiley.com](http://www.interscience.wiley.com).]

 <p><b>ade_n3</b></p>	 <p><b>HOMO</b></p>	 <p><b>HOMO-1</b></p>	 <p><b>HOMO-2</b></p>
KT	8.12	9.70	11.44
2 <sup>nd</sup> Order	7.96	8.54*	8.41
3 <sup>rd</sup> Order	8.32	9.47	10.74
OVGF	8.21	9.06	9.87
P3	8.48	9.31	9.80
$\Delta$ SCF[40]	8.25		
BP86/TZ2P[38]	8.28		
BP86/QZ4P[38]	8.20		
OVGF/TZVP[38]	8.04		
 <p><b>ade_n1</b></p>	 <p><b>HOMO</b></p>	 <p><b>HOMO-1</b></p>	 <p><b>HOMO-2</b></p>
KT	8.21	9.57	11.29
2 <sup>nd</sup> Order	8.08	8.54	8.18*
3 <sup>rd</sup> Order	8.45	9.39	10.59
OVGF	8.34	8.99	9.68
P3	8.62	9.28	9.61
$\Delta$ SCF[40]	8.42		
BP86/TZ2P[38]	8.30		
BP86/QZ4P[38]	8.21		
OVGF/TZVP[38]	8.06		



**TABLE IV**

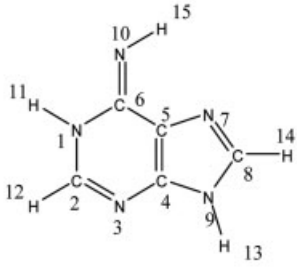
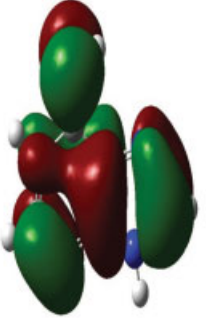
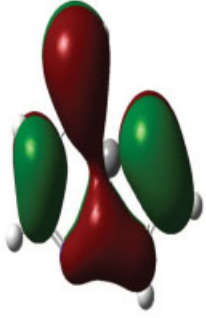
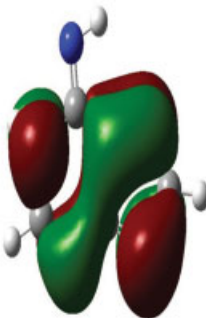
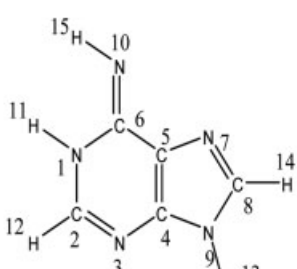



Vertical electron detachment energies of imi\_1\_n1\_n7 and imi\_2\_n1\_n7 tautomers with corresponding Dyson orbitals. [Color figure can be viewed in the online issue, which is available at [www.interscience.wiley.com](http://www.interscience.wiley.com).]

 <p><b>imi_1_n1_n7</b></p>	 <p><b>HOMO</b></p>	 <p><b>HOMO-1</b></p>	 <p><b>HOMO-2</b></p>
KT	8.26	10.75	11.44
2 <sup>nd</sup> Order	7.84	9.65	10.00
3 <sup>rd</sup> Order	8.28	10.36	10.94
OVGF	8.15	9.99	10.53
P3	8.38	10.33	10.72
BP86/TZ2P[38]	8.14		
BP86/QZ4P[38]	8.47		
OVGF/TZVP[38]	7.80		
 <p><b>imi_2_n1_n7</b></p>	 <p><b>HOMO</b></p>	 <p><b>HOMO-1</b></p>	 <p><b>HOMO-2</b></p>
KT	8.16	10.68	11.38
2 <sup>nd</sup> Order	7.80	9.57	9.92
3 <sup>rd</sup> Order	8.23	10.31	10.85
OVGF	8.10	9.93	10.45
P3	8.34	10.25	10.64
ΔSCF[40]	8.43		
BP86/TZ2P[38]	8.10		
BP86/QZ4P[38]	8.06		
OVGF/TZVP[38]	7.91		

\*Pole strength less than 0.85.

TABLE V

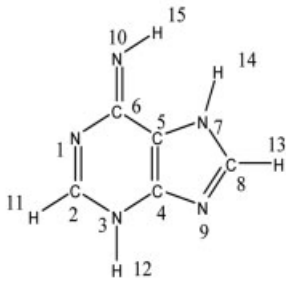
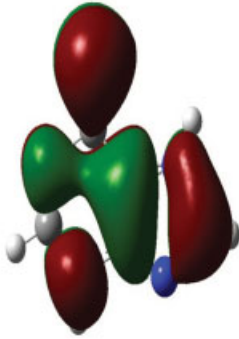
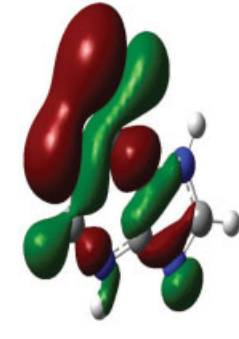
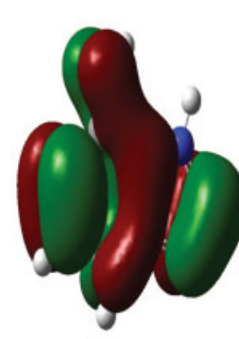
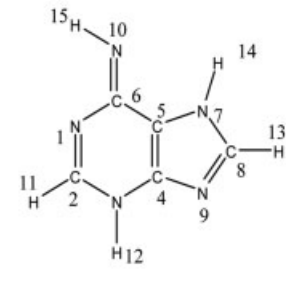
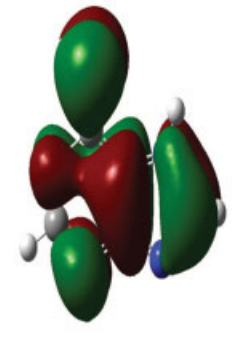
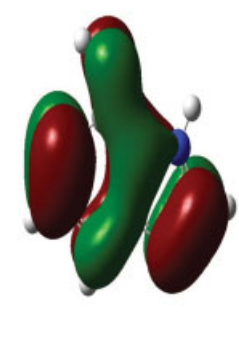
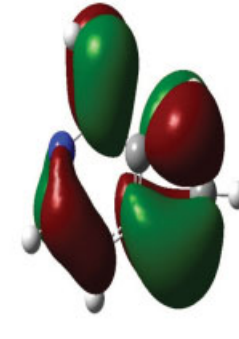
Vertical electron detachment energies of imi\_1\_n1\_n9 and imi\_2\_n1\_n9 tautomers with corresponding Dyson orbitals. [Color figure can be viewed in the online issue, which is available at [www.interscience.wiley.com](http://www.interscience.wiley.com).]

 <p><b>imi_1_n1_n9</b></p>	 <p><b>HOMO</b></p>	 <p><b>HOMO-1</b></p>	 <p><b>HOMO-2</b></p>
KT	7.99	10.93	11.30
2 <sup>nd</sup> Order	7.69	9.74	9.85
3 <sup>rd</sup> Order	8.08	10.55	10.73
OVGF	7.96	10.19	10.30
P3	8.22	10.38	10.62
ΔSCF[40]	8.27		
BP86/TZ2P[38]	7.96		
BP86/QZ4P[38]	7.88		
OVGF/TZVP[38]	7.76		
 <p><b>imi_2_n1_n9</b></p>	 <p><b>HOMO</b></p>	 <p><b>HOMO-1</b></p>	 <p><b>HOMO-2</b></p>
KT	7.94	10.86	11.24
2 <sup>nd</sup> Order	7.67	9.65	9.79
3 <sup>rd</sup> Order	8.05	10.50	10.64
OVGF	7.94	10.14	10.22
P3	8.19	10.30	10.54
BP86/TZ2P[38]	7.94		
BP86/QZ4P[38]	7.87		
OVGF/TZVP[38]	7.75		

\*Pole strength less than 0.85.

**TABLE VI**

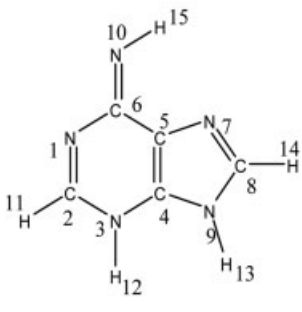
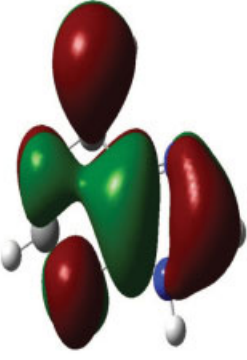
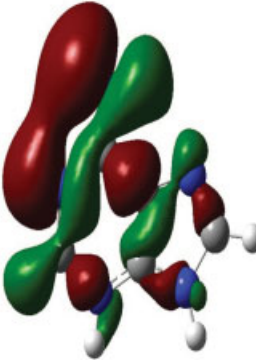
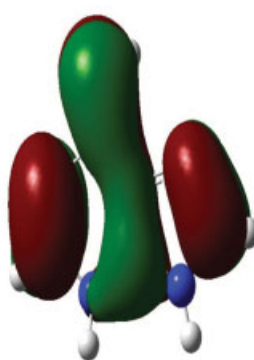
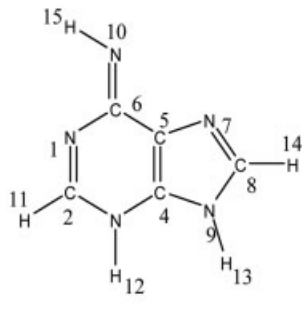
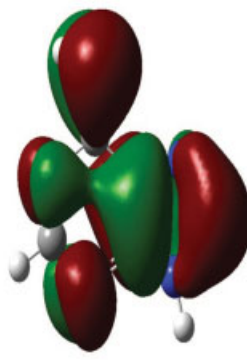
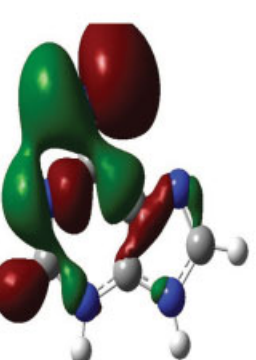
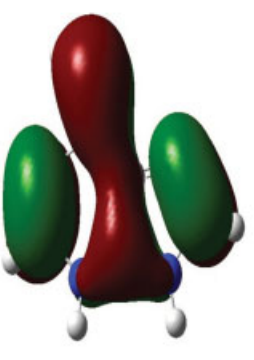
Vertical electron detachment energies of imi\_1\_n3\_n7 and imi\_2\_n3\_n7 tautomers with corresponding Dyson orbitals. [Color figure can be viewed in the online issue, which is available at [www.interscience.wiley.com](http://www.interscience.wiley.com).]

 <p><b>imi_1_n3_n7</b></p>	 <p><b>HOMO</b></p>	 <p><b>HOMO-1</b></p>	 <p><b>HOMO-2</b></p>
KT	8.21	11.08	10.57
2 <sup>nd</sup> Order	7.68	8.36	9.71
3 <sup>rd</sup> Order	8.18	10.29	10.32
OVGF	7.88	9.59	9.99
P3	8.25	9.52	10.31
BP86/TZ2P[38]	8.03		
BP86/QZ4P[38]	7.96		
OVGF/TZVP[38]	7.68		
 <p><b>imi_2_n3_n7</b></p>	 <p><b>HOMO</b></p>	 <p><b>HOMO-1</b></p>	 <p><b>HOMO-2</b></p>
KT	8.10	10.56	11.28
2 <sup>nd</sup> Order	7.60	9.64	9.92
3 <sup>rd</sup> Order	8.10	10.28	10.82
OVGF	7.96	9.94	10.43
P3	8.17	10.26	10.64
$\Delta$ SCF[40]	8.30		
BP86/TZ2P[38]	7.97		
BP86/QZ4P[38]	7.90		
OVGF/TZVP[38]	7.61		

\*Pole strength less than 0.85.

TABLE VII

Vertical electron detachment energies of imi\_1\_n3\_n9 and imi\_2\_n3\_n9 tautomers with corresponding Dyson orbitals. [Color figure can be viewed in the online issue, which is available at [www.interscience.wiley.com](http://www.interscience.wiley.com).]

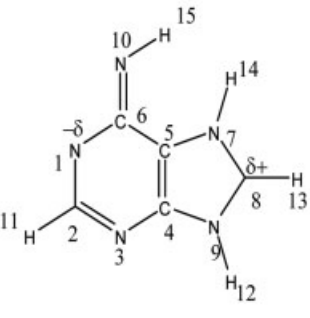
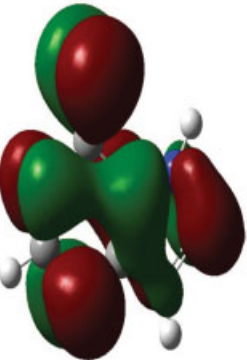
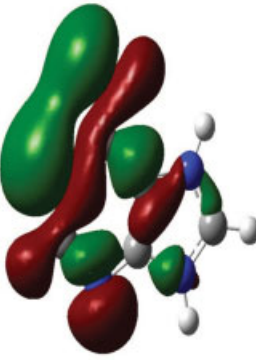
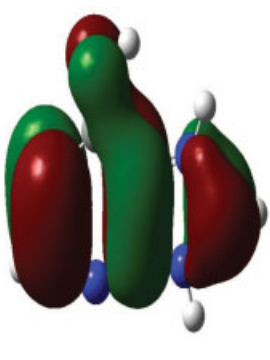
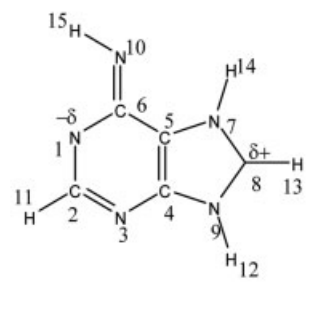
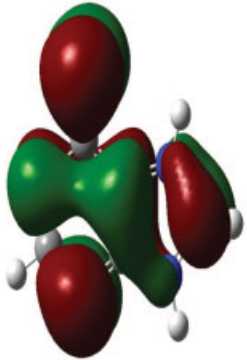
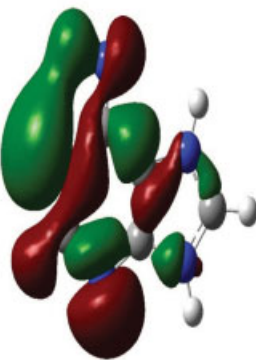
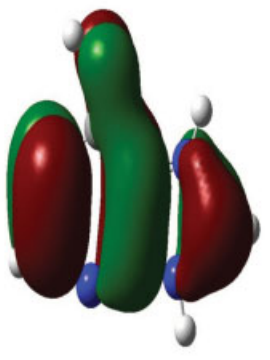
 <p>imi_1_n3_n9</p>	 <p>HOMO</p>	 <p>HOMO-1</p>	 <p>HOMO-2</p>
KT	8.02	10.86	10.58
2 <sup>nd</sup> Order	7.58	8.16	9.77
3 <sup>rd</sup> Order	8.03	10.00	10.39
OVGF	7.90	9.33	10.07
P3	8.13	9.26	10.33
BP86/TZ2P[38]	7.89		
BP86/QZ4P[38]	7.81		
OVGF/TZVP[38]	7.56		
 <p>imi_2_n3_n9</p>	 <p>HOMO</p>	 <p>HOMO-1</p>	 <p>HOMO-2</p>
KT	7.95	11.18	10.56
2 <sup>nd</sup> Order	7.53	8.39*	9.72
3 <sup>rd</sup> Order	7.97	10.31	10.36
OVGF	7.84	9.64	10.04
P3	8.07	9.48	10.28
$\Delta$ SCF[40]	8.30		
BP86/TZ2P[38]	7.84		
BP86/QZ4P[38]	7.77		
OVGF/TZVP[38]	7.50		

\*Pole strength less than 0.85.



**TABLE VIII**

Vertical electron detachment energies of imi\_1\_n7\_n9 and imi\_2\_n7\_n9 tautomers with corresponding Dyson orbitals. [Color figure can be viewed in the online issue, which is available at [www.interscience.wiley.com](http://www.interscience.wiley.com).]

 <p><b>imi_1_n7_n9</b></p>	 <p><b>HOMO</b></p>	 <p><b>HOMO-1</b></p>	 <p><b>HOMO-2</b></p>
KT	7.51	10.17	10.15
2 <sup>nd</sup> Order	6.82	7.45	9.39
3 <sup>rd</sup> Order	7.47	9.52	10.03
OVGF	7.15	8.75	9.67
P3	7.45	8.71	10.01
 <p><b>imi_2_n7_n9</b></p>	 <p><b>HOMO</b></p>	 <p><b>HOMO-1</b></p>	 <p><b>HOMO-2</b></p>
KT	7.47	10.56	10.14
2 <sup>nd</sup> Order	6.81	7.82*	9.33
3 <sup>rd</sup> Order	7.44	9.84	9.99
OVGF	7.13	9.05	9.63
P3	7.43	9.10	9.96

\*Pole strength less than 0.85.

and ionization energies for HOMO-1 and HOMO-2 are not available from non-EPT theoretical approaches. The HOMO and HOMO-2 Dyson orbitals

are of  $\pi$  type and resemble closely the  $6\pi$  and  $5\pi$  orbitals, whereas the HOMO-1 Dyson orbital has the same topological features as the  $29\sigma$  orbital seen



in the DFT calculations of Guerra et al. [38]. The  $\sigma$ -type HOMO-1 Dyson orbital has a large contribution from N lone-pair AOs. There is some marginal difference between density distributions of the Dyson orbitals depicted here and the Kohn-Sham DFT orbitals of Guerra et al. [38], but the disposition of nodal planes is similar. The near degeneracy of HOMO-1 and HOMO-2 is predicted by the P3 EPT approximant. The KT, second-order, third-order, and OVG results are not only different from the experimental values but also may give an incorrect ordering. The ADC(3) results [33] have the right ordering but are further different from experimental results.

The P3 first ionization energy of ade\_n7, which is also included in Table II, is 0.35 eV greater than the first ionization energy of ade\_n9, mirroring the higher total energy of ade\_n7 vis-à-vis ade\_n9. The HOMO and HOMO-2 of ade\_n7 are again  $\pi$ -type Dyson orbitals and the HOMO-1 Dyson orbital is of  $\sigma$  type with large contributions from N lone-pair AOs. The difference in orbital amplitudes on N9 and N7 between ade\_n7 and ade\_n9 reflects the change introduced by movement of H12 from N9 to N7. This effect is most visible for the HOMO-1  $\sigma$  orbital of ade\_n7 and ade\_n9 where the lone-pair contribution from the N-atom hosting H12 diminishes considerably in the  $\sigma$ -type HOMO-1 of ade\_n7. In both ade\_n9 and ade\_n7, corrections to the KT results are larger for the inner HOMO-2 and HOMO-1 orbitals as expected and underscore the need to calculate these through systematic perturbative improvements to avoid fortuitous resemblance between KT and P3 results for ade\_n7 HOMO. That correlation and relaxation effects play an important role that is easily brought out by the results tabulated here.

The results for tautomers ade\_n3 and ade\_n1 are presented in Table III. The main departure from ade\_n9 and ade\_n7 is the proton shift from the five-member ring to the N3 and N1 locations of the six-member ring for ade\_n3 and ade\_n1, respectively. As a consequence of this crowding of the six-member ring, the total energies go up. For HOMO-1 and HOMO-2, the orbital amplitudes shift markedly from the six-member ring to the five-member ring with appropriate redistribution of nodal topology and energetic reversal between the  $\pi$ -type and  $\sigma$ -type orbitals. For the  $\sigma$ -type HOMO-2, there is negligible participation from the atoms exclusive to the six-member ring and in the  $\pi$ -type HOMO-1, the contribution from the five-member ring dominates. The orbital shapes of HOMOs for ade\_n1, ade\_n3, ade\_n7, and ade\_n9

tautomers are quite similar, with the move of an H atom away from the five-member ring facilitating a less compact and thereby more loosely bound orbital. The ionization energies of ade\_n1 and ade\_n3 are therefore comparatively lower. The role of correlation and relaxation remains significant for the second-order results offer a somewhat misleading deep reduction to KT values. Moreover, the second-order binding energies of the  $\pi$ -type HOMO-1 for ade\_n3 and the  $\sigma$ -type HOMO-2 for ade\_n9 show pole strength values below 0.85, indicating a departure from the simple single orbital picture and indicating the need for a systematic investigation using third-order and P3-type higher order decouplings. The other topological details of these orbitals in terms of the number and orientation of nodal planes are similar to those discussed by Guerra et al. [38].

The results for imino tautomers are presented in Tables IV to VIII. The change from amino to imino forms changes the conjugation pattern and there is redistribution of two H atoms between the imino tautomers as opposed to one for their adenine counterparts. These two features control the energetic and orbital topology changes. Configurations with greater H crowding are higher in energy and those where the steric crowding is reduced (imi\_1\_n1\_n9) show improved relative stability. The conjugation patterns determine the details of the orbital amplitudes. Because all imino tautomers are energetically quite removed from the natural adenine base, the energetics of their first, second, and third ionization energies are not considered in the same detail as for the amine tautomers (ade\_n3 and ade\_n7) close to the neutral adenine base believed to assist in resolving spectral lines [34].

The HOMOs of the imino tautomers are similar to those of the amino tautomers except for more prominent contributions from the N10 lone pair and greater concentration on N1, which is more or less missing from the HOMOs of amino tautomers. Such shifts may be attributed to changes in conjugation patterns in the imino tautomers vis-à-vis their amino counterparts. The HOMO for all imino tautomers is quite similar both in terms of the P3 ionization energies and the corresponding Dyson orbital's density distribution (Table IV–VII). The greater instability of the zwitterionic tautomers (see Fig. 2) is reflected in the lower binding energy (Table VIII) for their HOMO, HOMO-1, and HOMO-2 and slightly larger/smaller electron density at the N1/C8 positions as expected. The HOMO-1 and HOMO-2 of imi\_1\_n1\_n7 and imi\_2\_n1\_n7 differ from each other (Table IV) in terms of  $\pi$ -orbital composition, with a

prominent role for imino N10 in HOMO-2, which is much less prominent in HOMO-1. The energy ordering of HOMO-1 and HOMO-2 is reversed vis-à-vis imi\_1\_n1\_n7 and imi\_2\_n1\_n7 in the case of imi\_1\_n1\_n9 and imi\_2\_n1\_n9 with HOMO-1 of imi\_1\_n1\_n9 and imi\_2\_n1\_n9 (Table V) showing gradual diminishing of orbital density on N3. In the case of imi\_1\_n3\_n7, the HOMO-2 (Table VI) is similar to the HOMO-1 of imi\_1\_n1\_n7 and imi\_2\_n1\_n7 (Table IV) but with a connected large-orbital amplitude on imino N. The HOMO-1 of imi\_1\_n3\_n7 in Table VI is a  $\sigma$  orbital with some similarity to  $\sigma$ -type HOMO-1 of ade\_n9 and ade\_n7 (Table II) and HOMO-2 of ade\_n3 and ade\_n1 (Table III) of the amino tautomers but with a larger, in-plane  $\pi$ -type contribution from the N1, C6, and N10 moiety facilitated by the change in conjugation pattern characterizing the imino tautomers. The HOMO and HOMO-1 (Table VI) of imi\_2\_n3\_n7 are similar to those of imi\_1\_n3\_n7, but imi\_1\_n3\_n7 has a  $\sigma$ -type HOMO-1, i.e., HOMO-1, HOMO-3 ordering of imi\_1\_n3\_n7 is reversed for the imi\_2\_n3\_n7 tautomer. The first two  $\pi$  orbitals of imi\_1\_n3\_n9, imi\_2\_n3\_n9 (Table VII), imi\_1\_n7\_n9, and imi\_2\_n7\_n9 (Table VIII) are similar to their counterparts of imi\_1\_n3\_n7 and imi\_2\_n3\_n7. However, HOMO-1 is  $\sigma$  type for imi\_1\_n3\_n9, imi\_1\_n7\_n9, and imi\_2\_n7\_n9, but is  $\pi$  type for imi\_2\_n3\_n9. Since the inner HOMOs are energetically close to each other, the exchange in ordering of HOMO-2 and HOMO-3 in the cases noted above is understandable and reinforces the need for using accurate methods such as the P3 EPT approximant used here.

#### 4. Concluding Remarks

Ionization energies from the use of many decouplings of the electron propagator theory on all 14 adenine tautomers using MP2/6-311++g(2df,p) optimized geometries have been presented and rationalized in terms of changes in structural features of the corresponding Dyson orbitals. The P3 results compare quite well with experimental results and the Dyson orbitals provide details responsible for the ordering of the first few ionization energies for all 14 adenine tautomers for the first time. The near similarity in value for first few ionization energies of structurally related tautomers has been mapped and points to the need for caution in resolution of PES for adenine and perhaps other nucleobases as well. The results presented here and also in our previous articles [62, 63] demonstrate the help that

can be rendered by electron propagator decouplings using systematically augmented basis sets in resolving PES spectra of biologically important molecules. The sometimes fortuitous agreement between Koopmans and experimental values and undue deep reductions by the second-order decoupling underscores the need for a systematic use of the higher third-order and P3 decouplings for accuracy and dependability in structural and energetic characterization of large molecules.

#### References

- Harris, V. H.; Smith, C. L.; Cummins, W. J.; Hamilton, A. L.; Adams, H.; Dickman, M.; Hornby, D. P.; Williams, D. M. *J. Mol. Biol.* 2003, 326, 1389.
- Florian, J.; Leszczynski, J. *J. Am. Chem. Soc.* 1996, 118, 3010.
- Ladik, J.; Förner, W. *The Beginnings of Cancer in the Cell*; Springer: Berlin, 1994.
- Miller, E. C. *Cancer Res.* 1978, 38, 1479.
- Leão, M. B. C.; Pavão, A. C. *Int. J. Quantum Chem.* 1997, 62, 323.
- Mohallem, J. R.; Vianna, R. O.; Quintao, A. D.; Pavão, A. C.; McWeeny, R. Z. *Phys. D.* 1997, 42, 135.
- Gu, J.; Xie, Y.; Schaefer, H. F. *J. Am. Chem. Soc.* 2005, 127, 1053.
- Plützer, Chr.; Nir, E.; de Vries, M. S.; Kleinermaans, K. *Phys. Chem. Chem. Phys.* 2001, 3, 5466.
- Piuzzi, F.; Mons, M.; Dimicoli, I.; Tardivel, B.; Zhao, Q. *Chem. Phys.* 2001, 270, 205.
- Nir, E.; Plützer, Chr.; Kleinermaans, K.; de Vries, M. *Eur. Phys. J. D.* 2002, 20, 317.
- Chin, W.; Dimicoli, I.; Piuzzi, F.; Tardivel, B.; Elhanine, M. *Eur. Phys. J. D.* 2002, 20, 347.
- Mons, M.; Dimicoli, I.; Piuzzi, F.; Tardivel, B.; Elhanine, M. *J. Phys. Chem. A.* 2002, 106, 5088.
- Sabio, M.; Topiol, S.; Lumma, W. C. *J. Phys. Chem.* 1990, 94, 1366.
- Carles, S.; Lecomte, F.; Schermann, J. P.; Desfrancois, C. *J. Phys. Chem. A.* 2000, 104, 10662.
- Salter, L. M.; Chaban, G. M. *J. Phys. Chem. A.* 2002, 106, 4251.
- Hanus, M.; Kabelac, M.; Rejnek, J.; Ryjacek, F.; Hobza, P. *J. Phys. Chem. B.* 2004, 108, 2087.
- Marian, C.; Nolting, D.; Weinkauff, R. *Phys. Chem. Chem. Phys.* 2005, 7, 3306.
- Hush, N. S.; Cheung, A. S. *Chem. Phys. Lett.* 1975, 34, 11.
- Lauer, G.; Schäfer, W.; Schweig, A. *Tetrahedron Lett.* 1975, 16, 3939.
- Dougherty, D.; Wittel, K.; Meeks, J.; McGlynn, S. P. *J. Am. Chem. Soc.* 1976, 98, 3815.
- Padva, A.; O'Donnell, T. J.; LeBreton, P. R. *Chem. Phys. Lett.* 1976, 41, 278.
- Dougherty, D.; McGlynn, S. P. *J. Chem. Phys.* 1977, 67, 1289.
- Padva, A.; Peng, S.; Lin, J.; Shahbaz, M.; LeBreton, P. R. *Biopolymers* 1978, 17, 1523.

24. Lin, J.; Yu, C.; Peng, S.; Akiyama, I.; Li, K.; Lee, K. L.; Lebreton, P. R. *J Am Chem Soc* 1978, 100, 2303.
25. Lin, J.; Yu, C.; Peng, S.; Akiyama, I.; Li, K.; Lee, K. L.; Lebreton, P. R. *J Phys Chem* 1980, 104, 1006.
26. Kubota, M.; Kobayashi, T. *J Electron Spectrosc Relat Phenom* 1996, 82, 61.
27. Lifschitz, C.; Bergmann, E. D.; Pullman, B. *Tetrahedron Lett* 1967, 46, 4583.
28. Peng, S.; Padva, A.; Lebreton, P. R. *Proc Natl Acad Sci U S A* 1976, 73, 2966.
29. Dougherty, D.; Younathan, E. S.; Voll, R.; Abdunur, S.; McGlynn, S. P. *J Electron Spectrosc Relat Phenom* 1978, 13, 379.
30. Lin, J.; Yu, C.; Peng, S.; Akiyama, I.; Li, K.; Lee, K. L.; LeBreton, P. R. *J Am Chem Soc* 1980, 102, 4627.
31. Urano, S.; Yang, X.; Le Breton, P. R. *J Mol Struct* 1989, 214, 315.
32. Alyoubi, A. O.; Hilal, R. O. *J Biophys Chem* 1995, 55, 231.
33. Trofimov, A. B.; Schirmer, J.; Kobychiev, V. B.; Potts, A. W.; Holland, D. M. P.; Karlsson, L. *J Phys B At Mol Opt Phys* 2006, 39, 305.
34. Plützer, C.; Kleinerhanns, K. *Phys Chem Chem Phys* 2002, 4, 4877.
35. Laxer, A.; Major, D. T.; Gottlieb, H. E.; Fischer, B. *J Org Chem* 2001, 66, 5463.
36. De Voe, H.; Tinoco, I. *J Mol Biol* 1962, 4, 500.
37. Crespo-Hernández, C. E.; Arce, R.; Ishikawa, Y.; Gorb, L.; Leszczynski, J.; Close D. M. *J Phys Chem A* 2004, 108, 6373.
38. Guerra, C. F.; Bickelhaupt, F. M.; Saha, S.; Wang, F. *J Phys Chem A* 2006, 110, 4012.
39. Guerra, C. F.; Bickelhaupt, F. M.; Snijders, J. G.; Baerends, E. J. *Chem Eur J* 1999, 5, 3581.
40. Leão, M. B. C.; Longo, R. L.; Pavão, A. C. *J Mol Struct (Theochem)* 1999, 490, 145.
41. Dolgounitcheva, O.; Zakrzewski, V. G.; Ortiz, J. V. *Int J Quantum Chem* 2000, 80, 831.
42. Preuss, M.; Schmidt, W. G.; Seino, K.; Furthmüller, J.; Bechstedt, F. *J Comput Chem* 2003, 25, 112.
43. Wetmore, S. D.; Boyd, R. J.; Eriksson, L. A. *J Phys Chem B* 1998, 102, 10612.
44. Wetmore, S. D.; Boyd, R. J.; Eriksson, L. A. *Chem Phys Lett* 2002, 322, 129.
45. Improta, R.; Scalmani, G.; Barone V. *Int J Mass Spectrom* 2000, 201, 321.
46. Satzger, H.; Townsend, D.; Stolow, A. *Chem Phys Lett* 2006, 430, 144.
47. Satzger, H.; Townsend, D.; Zgierski, M. Z.; Patchkovskii, S.; Ullrich, S.; Stolow, A. *Proc Natl Acad Sci U S A* 2006, 103, 10196.
48. Roca-Sanjuán, D.; Rubio, M.; Merchán, M.; Serrano-Andrés, L. *J Chem Phys* 125:084302, 2006.
49. Von Niessen, W.; Schirmer, J.; Cederbaum, L. S. *Comput Phys Rep* 1984, 1, 57.
50. Cederbaum, L. S.; Domcke, W.; Schirmer, J.; Von Niessen, W. *Adv Chem Phys* 1986, 65, 115.
51. Ortiz, J. V. *J Chem Phys* 1996, 104, 7599.
52. Ortiz, J. V.; Zakrzewski, V. G.; Dolgounitcheva, O. In *Conceptual Trends in Quantum Chemistry*; Kryachko, E. S., Ed.; Kluwer: Dordrecht, 1997; Vol. 3, p 465.
53. Linderberg J.; Öhrn, Y. *Propagators in Quantum Chemistry*, 2nd ed.; Wiley, Hoboken: New Jersey, 2004.
54. Cederbaum, L. S.; Domke, W. *Adv Chem Phys* 1977, 36, 205.
55. Simons, J. *Ann Rev Phys Chem* 1977, 28, 15.
56. Öhrn, Y.; Born, G. *Adv Quant Chem* 1981, 13, 1.
57. Ortiz, J. V. *Adv Quantum Chem* 1999, 33, 35.
58. Mishra, M. K.; Medikeri, M. N. *Adv Quantum Chem* 1996, 27, 225.
59. Ortiz, J.V. In *Computational Chemistry: Reviews of Current Trends*, Leszczynski, J., Ed.; World Scientific: Singapore, 1997; Vol 2, p 1.
60. Schirmer, J.; Cederbaum, L. S.; Walter, O. *Phys Rev A* 1983, 28, 1237.
61. Frisch, M. J.; Trucks, G. W.; Schlegel, H.; Scuseria, G. E.; Robb, M. A.; Cheeseman, J. R.; Montgomery, J. A. Jr.; Vreven, T.; Kudin, K. N.; Burant, J. C.; Millam, J. M.; Iyengar, S. S.; Tomasi, J.; Barone, V.; Mennucci, B.; Cossi, M.; Scalmani, G.; Rega, N.; Petersson, G. A.; Nakatsuji, H.; Hada, M.; Ehara, M.; Toyota, K.; Fukuda, R.; Hasegawa, J.; Ishida, M.; Nakajima, T.; Honda, Y.; Kitao, O.; Nakai, H.; Klene, M.; Li, X.; Knox, J. E.; Hratchian, H. P.; Cross, J. B.; Adamo, C.; Jaramillo, J.; Gomperts, R.; Stratmann, R. E.; Yazyev, O.; Austin, A. J.; Cammi, R.; Pomelli, C.; Ochterski, J. W.; Ayala, P. Y.; Morokuma, K.; Voth, G. A.; Salvador, P.; Dannenberg, J. J.; Zakrzewski, V. G.; Dapprich, S.; Daniels, A. D.; Strain, M. C.; Farkas, O.; Malick, D. K.; Rabuck, A. D.; Raghavachari, K.; Foresman, J. B.; Ortiz, J. V.; Cui, Q.; Baboul, A. G.; Clifford, S.; Cioslowski, J.; Stefanov, B. B.; Liu, G.; Liashenko, A.; Piskorz, P.; Komaromi, I.; Martin, R. L.; Fox, D. J.; Keith, T.; Al-Laham, M. A.; Peng, C. Y.; Nanayakkara, A.; Challacombe, M.; Gill, P. M. W.; Johnson, B.; Chen, W.; Wong, M. W.; González, C.; Pople, J. A. *Gaussian03, Revision B. 03*, Gaussian, Inc.: Pittsburgh, PA, 2003.
62. Melin, J.; Mishra, M. K.; Ortiz, J. V. *J Phys Chem A* 2006, 110, 12231.
63. Melin, J.; Singh, R. K.; Mishra, M. K.; Ortiz, J. V. *J Phys Chem A* 2007, 111, 13069.